

**AN EXPERIMENTAL INVESTIGATION OF DAMAGE  
RESISTANCE AND DAMAGE TOLERANCE  
OF COMPOSITE MATERIALS**

**FINAL REPORT**

**R.Prabhakaran  
Principal Investigator  
Department of Mechanical Engineering  
Old Dominion University  
Norfolk, VA 23529**

**NASA Research Grant No. NAG8-1813 (ODURF # 113381)**

**Marshall Space Flight Center, AL 35812**

**March 12, 2003**

# **AN EXPERIMENTAL INVESTIGATION OF DAMAGE RESISTANCE AND DAMAGE TOLERANCE OF COMPOSITE MATERIALS**

**R. Prabhakaran  
Old Dominion University**

## **INTRODUCTION**

The project included three lines of investigation, aimed at a better understanding of the damage resistance and damage tolerance of pultruded composites. The three lines of investigation were: (i) measurement of permanent dent depth after transverse indentation at different load levels, and correlation with other damage parameters such as damage area (from x-radiography) and back surface crack length, (ii) estimation of point stress and average stress characteristic dimensions corresponding to measured damage parameters, and (iii) an attempt to measure the damage area by a reflection photoelastic technique. All the three lines of investigation were pursued and the results are summarized below.

### **(i) Permanent Indentation Depth:**

While a large body of literature is available regarding the response of composites subjected to low velocity impact or quasi-static transverse loading, very limited information is available for pultruded composites.

The specimen preparation, test fixture and the overall experimental procedure was very similar to the work done and reported earlier [1] and is not repeated in detail here. Only the important features are summarized. The pultruded composite specimens were fabricated from sheets of two thicknesses: 6.3 mm and 12.7 mm. The 6.3 mm thick specimens were of 152 mm length and 102 mm width. The 12.7 mm thick specimens were 254 mm length and 178 mm width. The quasi-static indentation tests were performed on a Tinius-Olsen electromechanical (hydraulic-screwdriven) machine. A completely new specimen holder and fixture was fabricated.

The 6.3 mm thick specimens were positioned and centered on a supporting plate with a 51 mm square cutout; they were loaded by a 19 mm diameter steel spherical indenter. The 12.7 mm thick specimens were positioned and centered on a supporting plate with a 102 mm square cutout; they were loaded centrally by a 38 mm diameter spherical steel indenter. Two DCDT's (direct current differential transformers) were used to measure the indenter movement and the central displacement of the specimen. The load and displacements were recorded with a data acquisition system [1]. The test set-up is shown in Fig. 1.

The depth of indentation (permanent: remaining after the indentation force is removed) was measured using a DCDT whose resolution was 0.0007mm. This measurement was performed 24 hours after the indentation test and thus represented the equilibrium conditions. On flat specimens, the DCDT was moved along the two perpendicular directions along orthogonal diameters of the indentation. Several measurements were made and an average depth was recorded.

Compression tests were conducted on composite specimens with a series of circular holes, specimens that were subjected to different levels of transverse indentation loads and specimens that had no holes and not subjected to any prior loading. The end-gripped compression test fixture used for this investigation is described in detail [1] and shown in Fig. 2. By comparing the compressive strength of specimens with circular holes and the compressive strength of specimens subjected to quasi-static transverse indentation loads, an 'equivalent hole diameter' was found. The test results are summarized in two figures. These results represent those reported in [1] and additional tests performed to verify and supplement them. The first, Fig. 3, shows the compressive strength as a function of the indentation depth. It is seen from this figure that for both the thicknesses, there is a non-linear relationship between the compressive strength and the

dent depth. A single curve appears to fit all the points. The second figure, Fig. 4, shows the variation of the 'equivalent hole diameter' with the indentation depth. Again, a single curve appears to fit the results for both the thicknesses.

(ii) Point-Stress and Average-Stress Characteristic Dimensions:

The effect of geometrical discontinuities, such as circular holes, on the strength of composites has been investigated by many researchers. One of the methods of investigation has been on the lines of Neuber's elementary block theory for metallic materials. Here, a point-stress characteristic dimension or average-stress characteristic dimension is determined from the notched and unnotched strengths. There has been a robust discussion by researchers regarding the constancy of these two characteristic dimensions and regarding their dependence on the hole size itself. The principal investigator has been one of the researchers [2, 3] to show that the dimensions do depend on the notch size.

While most of the work performed in this area has been with the  $0^\circ$  orientation of composites and in the tensile mode, the current work was mainly on the comparison of the tensile and compressive behavior. Directions parallel and perpendicular to the pultrusion direction have also been considered at least for the tensile loading. A large number of specimens have been tested in tension and compression, for a range of hole sizes. For tension, the specimen widths ranged from 25 to 62.5 mm, with hole radii ranging from 1.27 mm to 15.875 mm. For compression, the ratio of the hole diameter to specimen width varied from 0.07 to 0.65. In each case, three identical tests were conducted and the results were averaged. The procedure for extracting  $d_0$ , the point-stress characteristic dimension, and  $a_0$ , the average-stress characteristic dimension, are standard and is explained in many publications [2, 3, 4, 5]. The results are summarized here.

The variation of the point-stress characteristic dimension,  $d_o$ , and the average-stress characteristic dimension,  $a_o$ , in tension for the  $0^\circ$  (parallel to the pultruded direction) and the  $90^\circ$  (perpendicular to the pultrusion direction) orientations is shown in Fig. 5. While scatter is to be expected in such results, the results for the average-stress dimension appear to show more scatter. Both  $d_o$  and  $a_o$  increase with the hole size and  $a_o$  is significantly larger than  $d_o$ , for a given orientation (as should be expected, based on the definitions of the characteristic dimensions).

The variation of the point-stress characteristic dimension,  $d_o$ , and the average-stress characteristic dimension,  $a_o$ , in compression for the  $0^\circ$  (parallel to the pultrusion direction) orientation for two thicknesses of the compression specimens, is shown in Fig. 6. These are the same two thicknesses mentioned earlier, namely 6.3 mm and 12.7 mm. Similar observations can be made in the case of this figure as for the previous figure. The scatter for the  $a_o$  values is significantly larger than for  $d_o$ . Both the characteristic dimensions increase with the size of the hole. And  $a_o$  is larger than  $d_o$ . The consolidated results are shown in Fig. 7. Here, the tension (denoted as T) and compression (denoted as C) results are shown, without the individual points. Only the best-fitting lines are shown. It is seen here that the characteristic dimensions are larger for the compressive loading, compared to the tensile loading.

### (iii) Reflection Photoelasticity:

The techniques of reflection photoelasticity, employing photoelastic coatings, are well established [6]. In most of the applications, the photoelastic coatings are bonded to materials (mostly metals, but occasionally composites also) and the stresses or strains in the structure are obtained in in-plane loading. Such in-plane loading produces mostly elastic stresses and strains, relatively small in magnitude. But in the current context, it was decided to explore the possibility

of utilizing the reflection photoelastic technique to give some indication of the stresses/damage remaining (residual) after the quasi-static transverse loading. On the smaller (152mm×102 mm×6.3 mm) pultruded composite specimens, photoelastic coating pieces of size 50 mm square were bonded on the top face (the side loaded by the indenter) and 44 mm×44 mm pieces were bonded on the opposite side. To accommodate the indenter, a large hole was machined in the coating bonded to the top face (before bonding). On the larger (254 mm×178mm×12.7 mm) pultruded composite specimens, photoelastic coating pieces of size 100 mm square were bonded on the top face (the side loaded by the indenter) and 87 mm×87mm pieces were bonded on the opposite face. To accommodate the indenter, a large hole was machined in the coating bonded to the top face (before bonding). The adhesive used for bonding the photoelastic coating to the composite contained aluminum powder, to enhance the light-reflecting characteristic. Several specimens of each size were prepared. Six specimens of the 6.3 thickness were loaded to different load levels (transverse loading) and unloaded; these loads were, 6.9 kN, 4.0 kN, 4.9 kN, 5.8 kN, 6.7 kN and 7.3 kN. Six specimens of the 12.7 mm thickness were also loaded to different load levels (transverse loading) and unloaded; these loads were, 18.5 kN, 11.5 kN, 13.1 kN, 15.6 kN, 16.8 kN and 18.7 kN. All the specimens were examined through a reflection polariscope using polychromatic light.

One of the specimens with the bonded photoelastic coating is shown in Fig. 8. The specimen, located on the loading fixture and ready to be loaded in transverse bending, is shown in Fig. 9. As mentioned earlier, the coating on the loading face had a circular hole to accommodate the indenter. A close-up view of another (larger) specimen is shown in Fig. 10. After loading and unloading, the coating on the loaded face exhibited residual isochromatic fringe pattern, as shown in Fig. 11. This figure is typical for all the tested specimens. A typical

residual isochromatic fringe pattern on the bottom face is shown in Fig. 12. The isochromatic fringe patterns lacked the clarity and the definition needed for any quantitative measurements; an additional problem was the necessity to use polychromatic light instead of monochromatic light.

During the experiments, it was observed that the photoelastic coating separated from the composite specimen at relatively high loads. This was due to the failure of the adhesive, which appeared to be relatively brittle. A very interesting observation was that the adhesive, after the photoelastic coating separation, exhibited interesting crack patterns. Cracks at a relatively smaller load and higher load are shown in Figs. 13 and 14, respectively. For future work, it should be interesting to compare the damage in the composite assessed by cracks in the composite itself and cracks in the adhesive.

## CONCLUSIONS

All the three objectives of the investigation were met. The indenter induced permanent indentation depth was measured and correlated with the composite damage through the equivalent hole diameter concept. The point-stress and average-stress characteristic dimensions were investigated in tension and compression and compared. An attempt was made to assess the damage due to quasi-static transverse indentation by bonding photoelastic coatings.

## ACKNOWLEDGEMENT

The assistance of Dr. M. C. Saha and Mr. H. Xu is greatly appreciated; both were graduate students at the time. The help of the personnel in the Machine Shop is also gratefully acknowledged. Mr. Tom Galloway helped in many ways also.

## REFERENCES

1. Elastic Properties, Strength and Damage Tolerance of Pultruded Composites, M. C. Saha, Ph.D. Thesis, Mechanical Engineering Department, Old Dominion University, 2001.
2. Tensile Fracture of Composites with Circular Holes, R. Prabhakaran, Materials Science and Engineering, Vol. 41, pp. 121-125 (1979).
3. Hole-Size Effects in Pultruded Composites, R. Prabhakaran, H. Xu, Mechanics of Composite Materials, Vol. 37, No. 1, pp. 79-84 (2001).
4. Notched Strength of Composite Materials, R. B. Pipes, R.C. Wetherhold, J. W. Gillespie, Journal of Composite Materials, Vol. 13, pp. 148-160 (1979).
5. Notched Strength and Fracture Criterion in Fabric Composite Plates Containing a Circular Hole, J. K. Kim, D. S. Kim, N. Takeda, Journal of Composite Materials, Vol. 29, No. 7, pp. 982-998 (1995).
6. Experimental Stress Analysis, J. W. Dally and W. F. Riley, McGraw Hill, 3<sup>rd</sup> Edition, 1991.

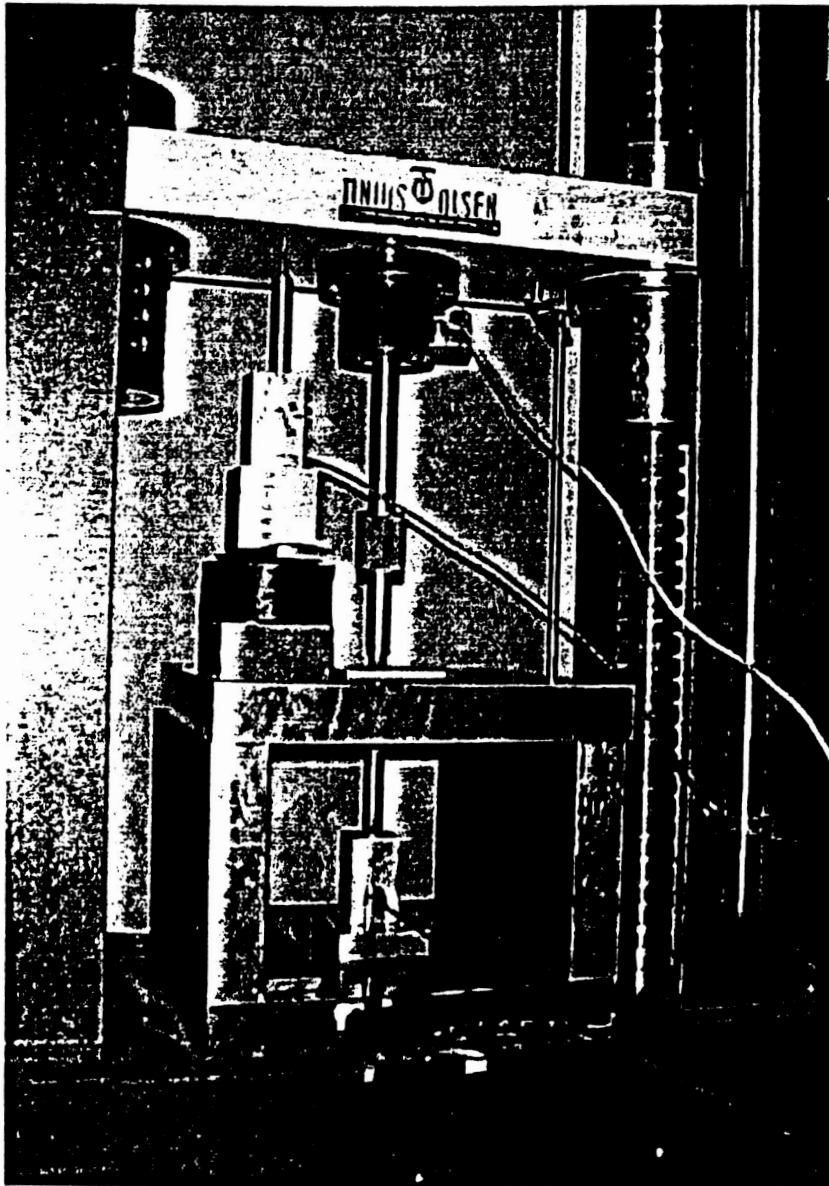


Figure 1: Photograph of the quasi-static indentation test setup

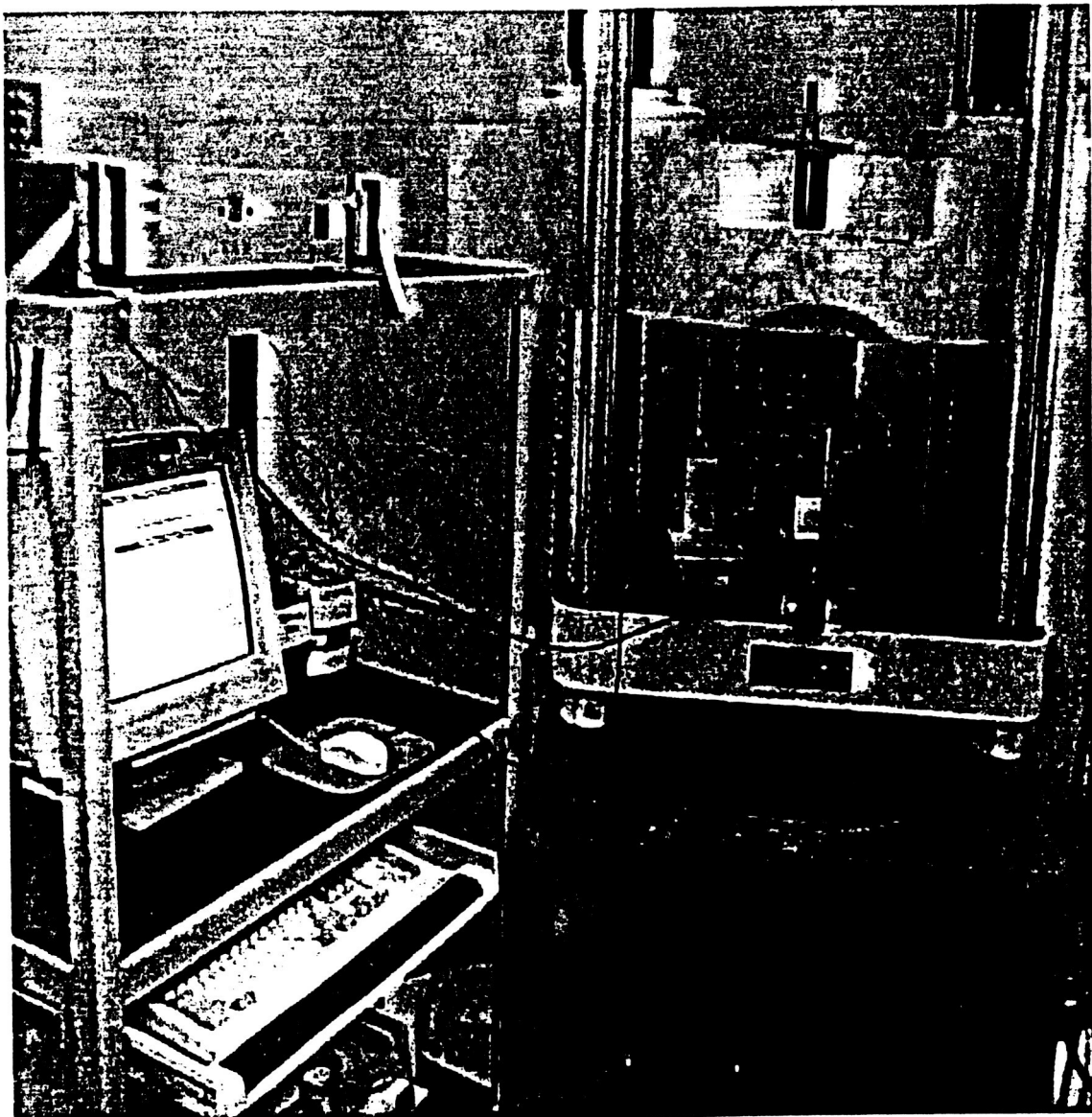


Figure 2: Compression testing set-up

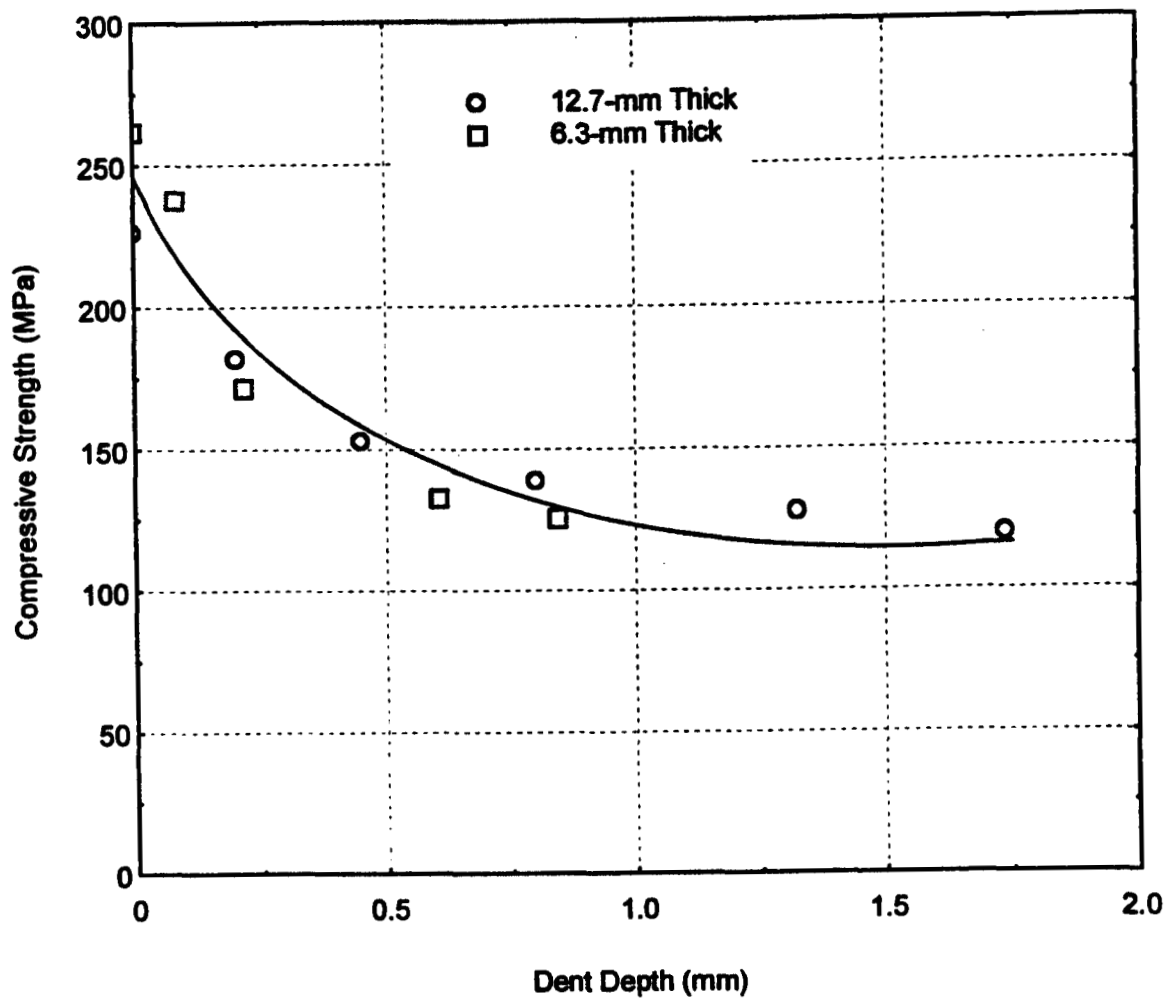


Figure 3: Compressive strength as a function of dent depth

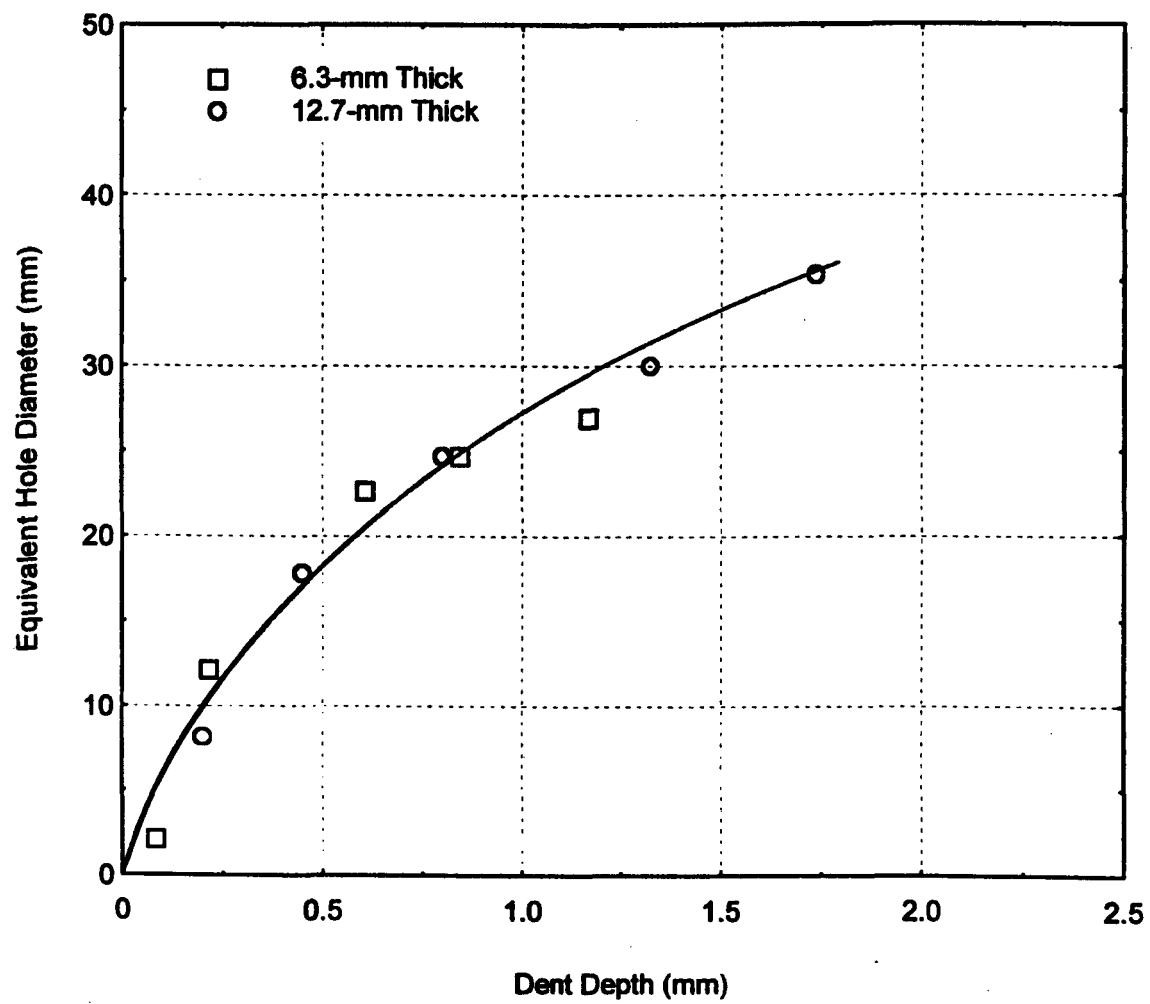


Figure 4: 'Equivalent hole diameter' as a function of the dent depth

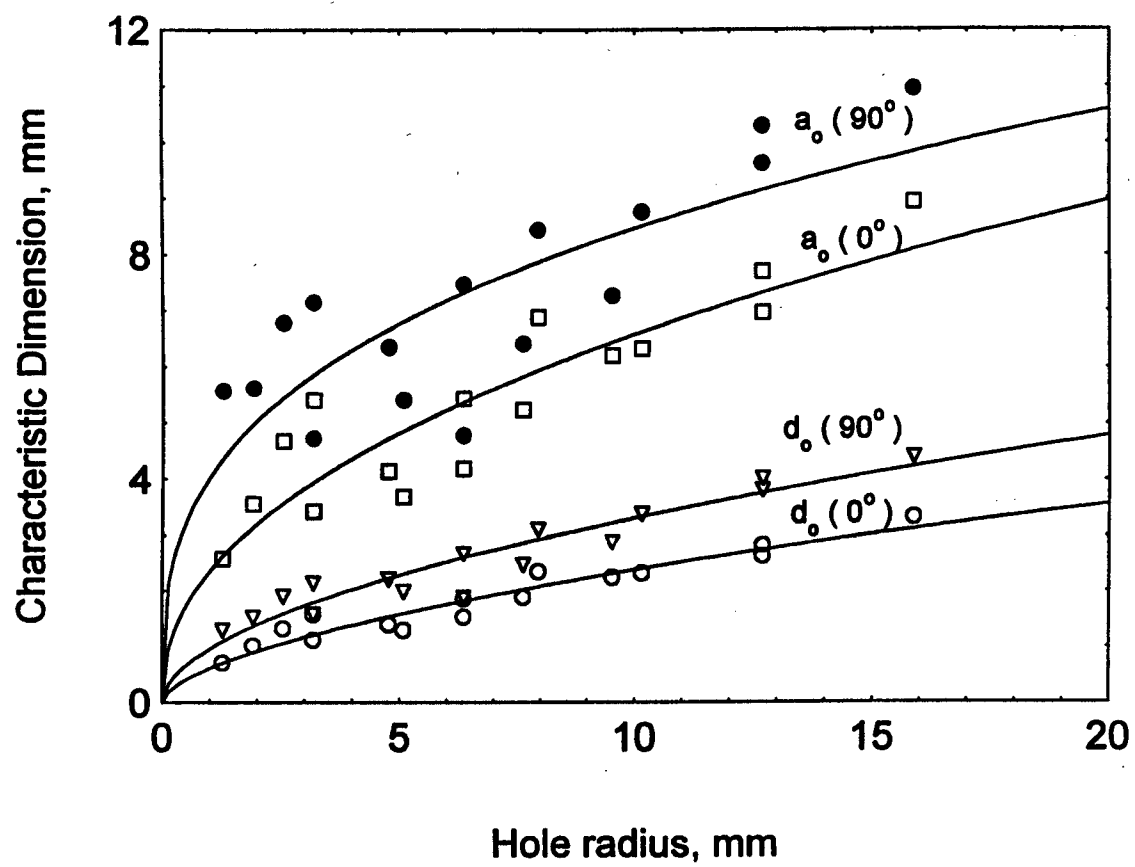


Figure 5: Characteristic dimensions in tension for the 0-degree and 90-degree orientations

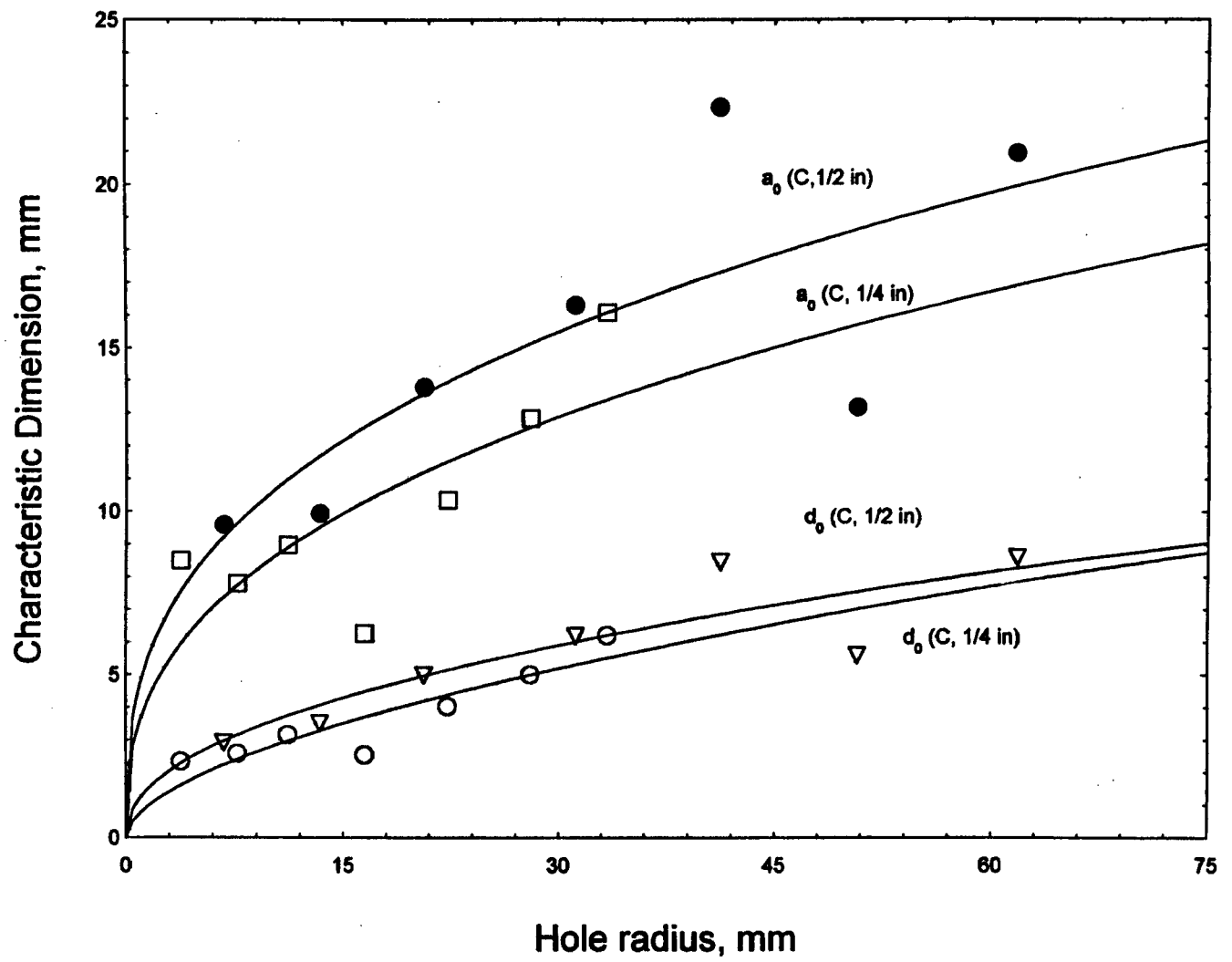


Figure 6: Characteristic dimensions in compression for two specimen thicknesses

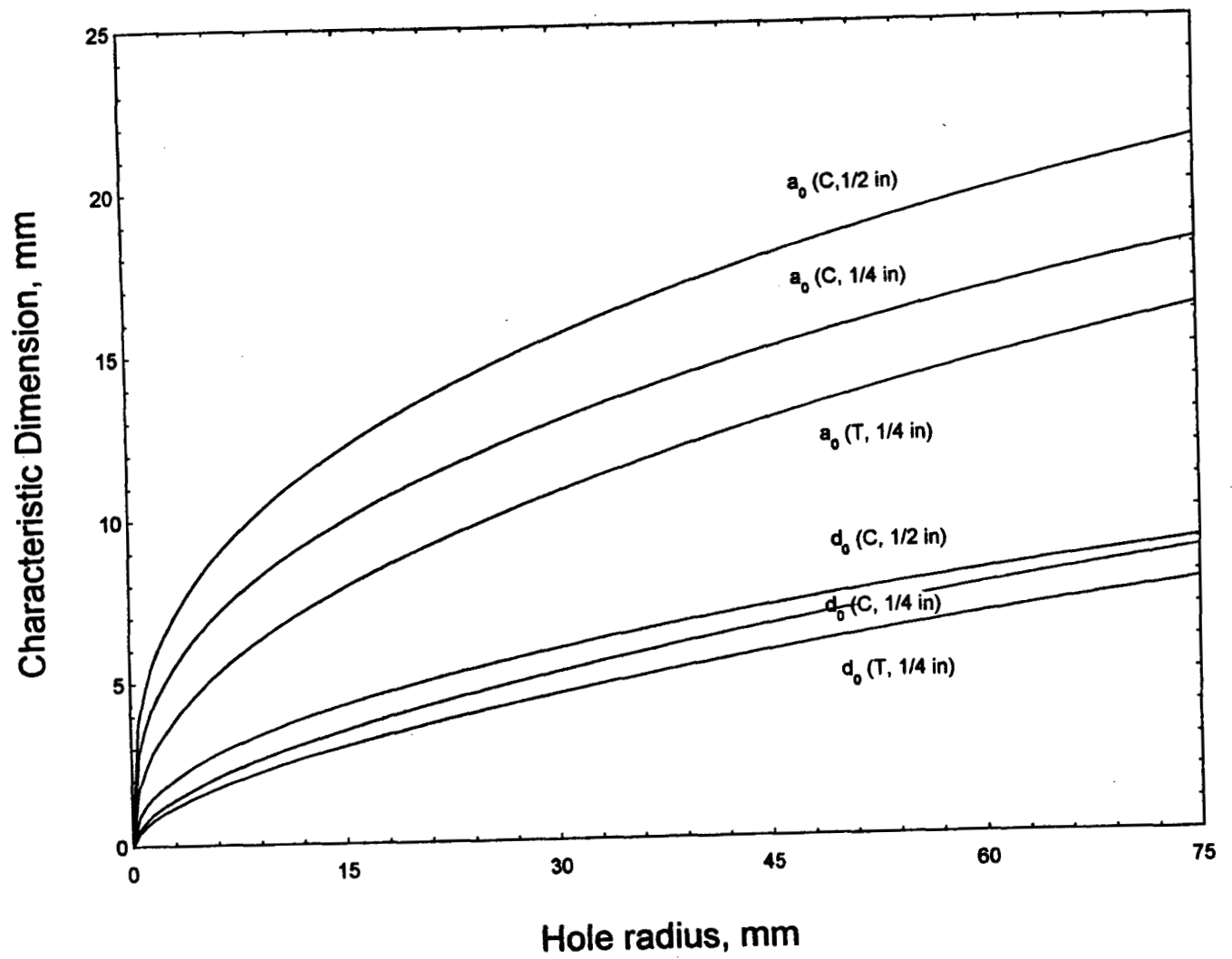


Figure 7: Consolidated results for characteristic dimensions in tension and compression

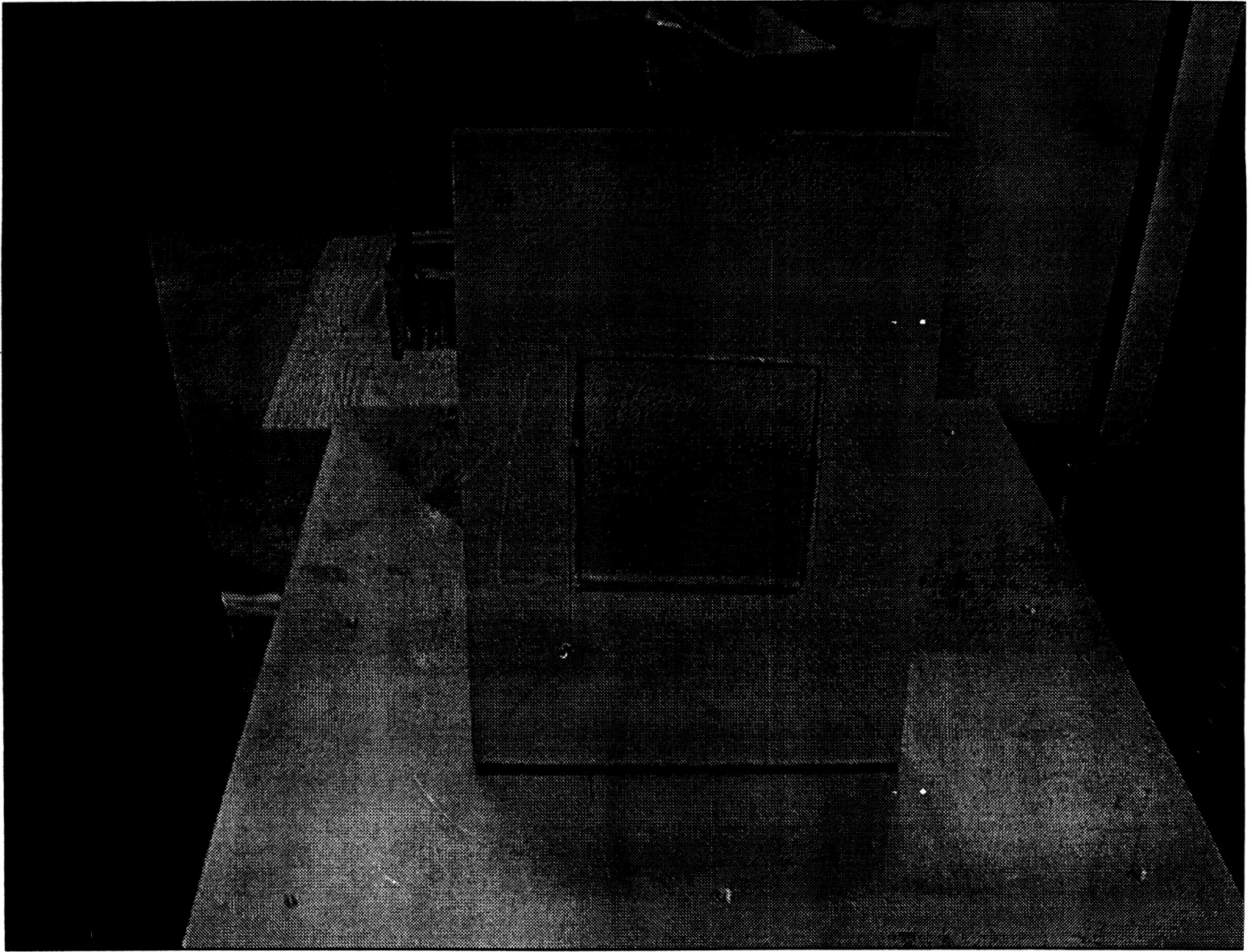


Figure 8: Pultruded composite specimen with the photoelastic coating

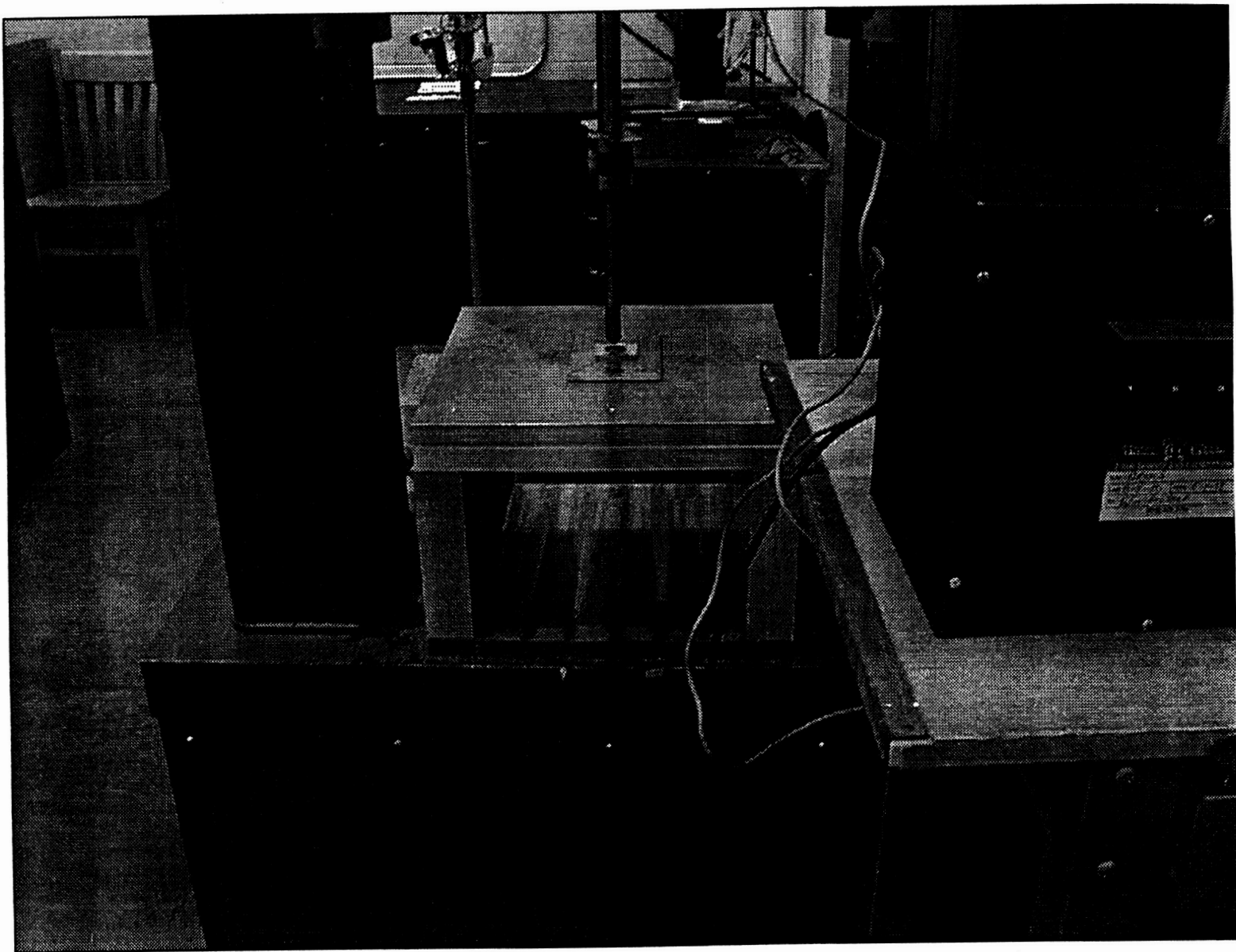


Figure 9: Composite specimen with the photoelastic coating in the test fixture

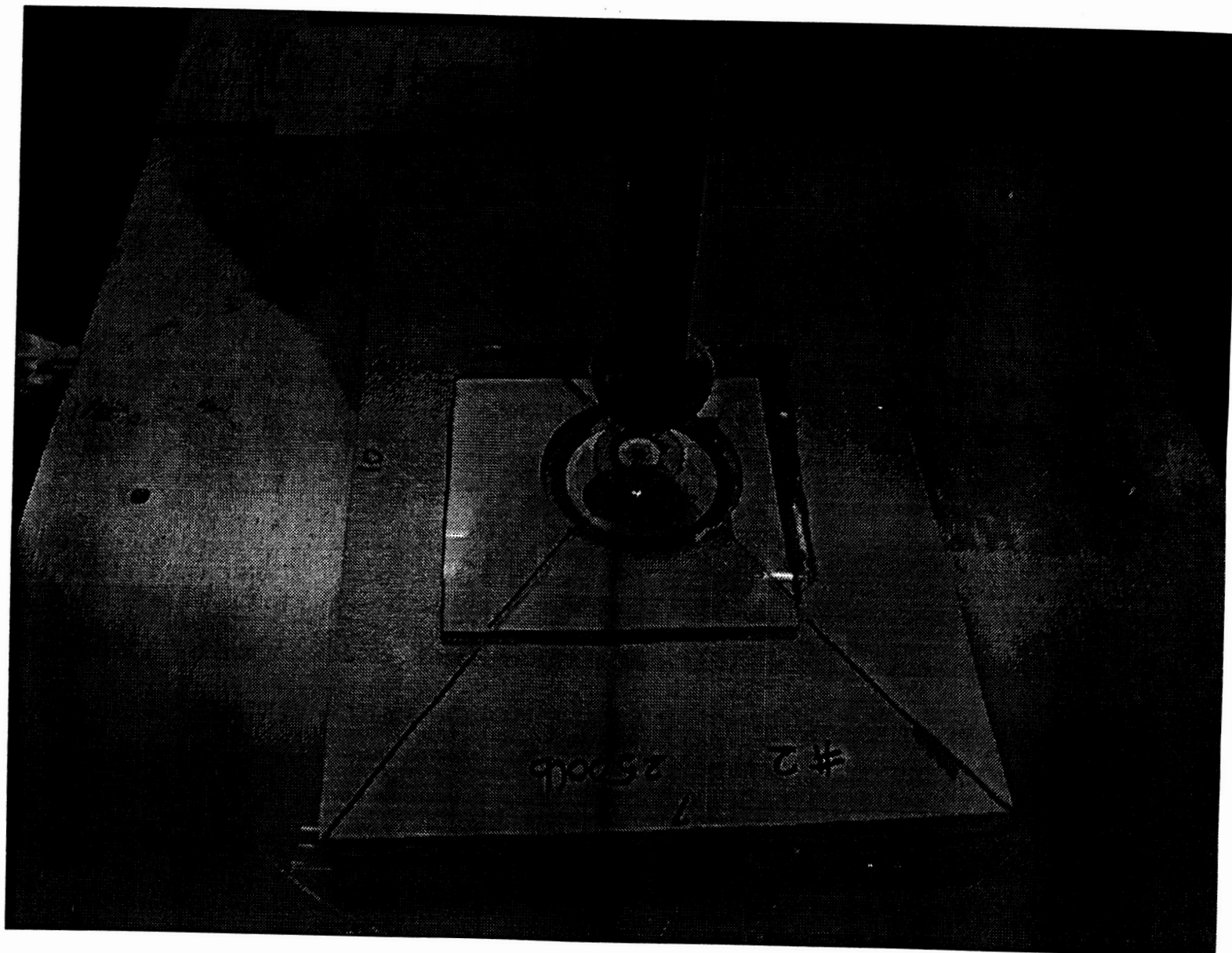


Figure 10: Close-up view of the composite specimen, with the indenter in position

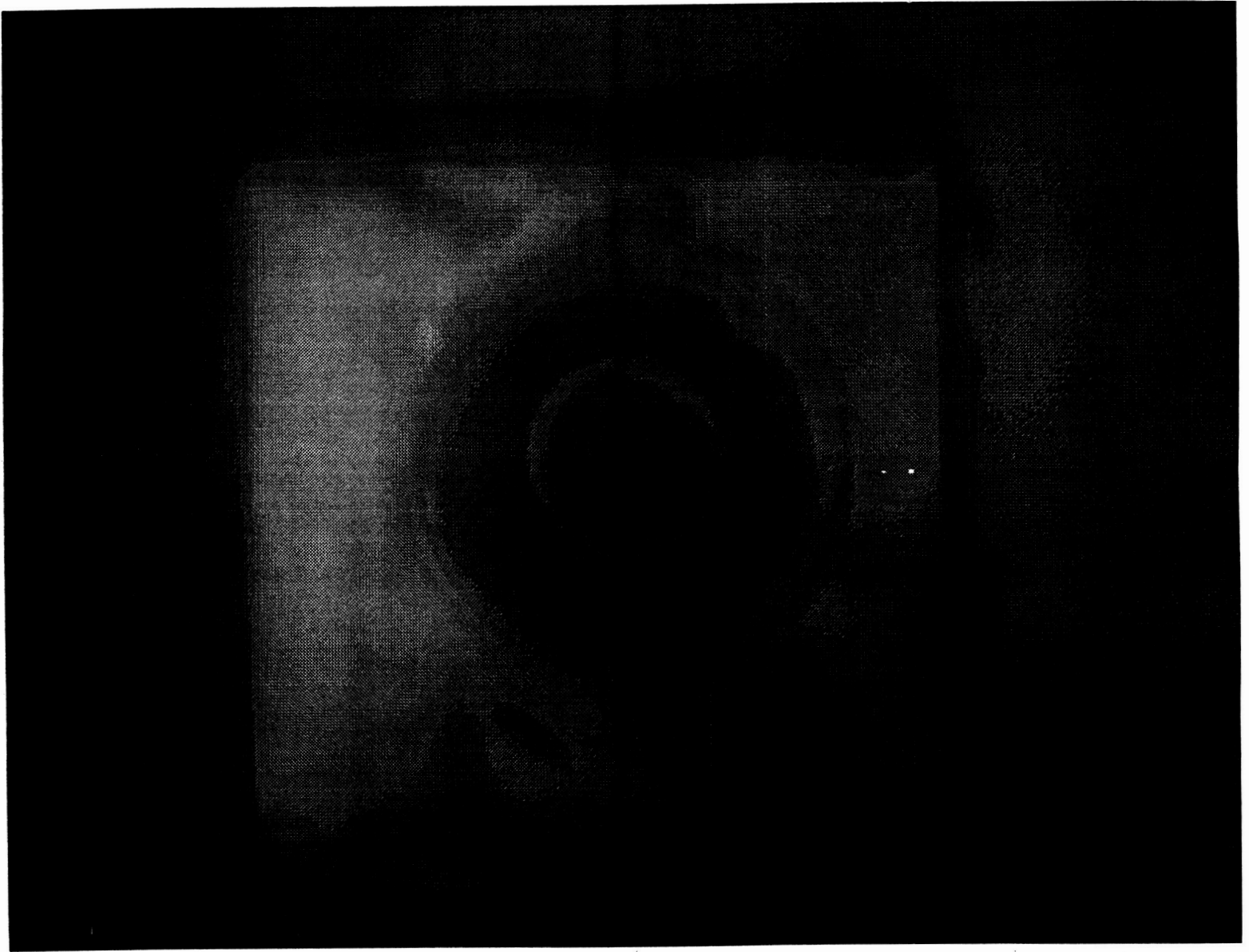


Figure 11: Residual isochromatic fringe pattern on the loaded face

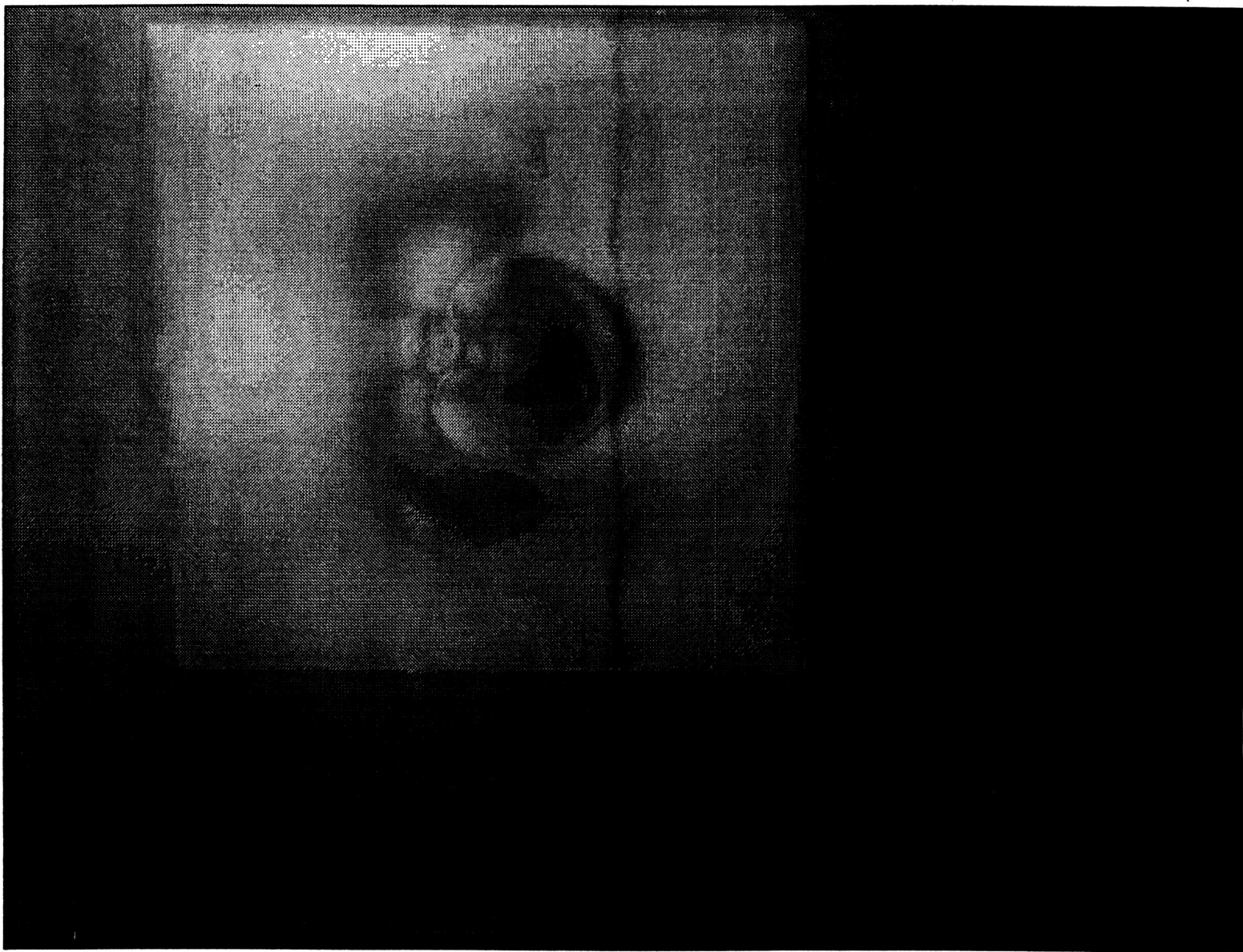


Figure 12: Residual isochromatic fringe pattern on the bottom face

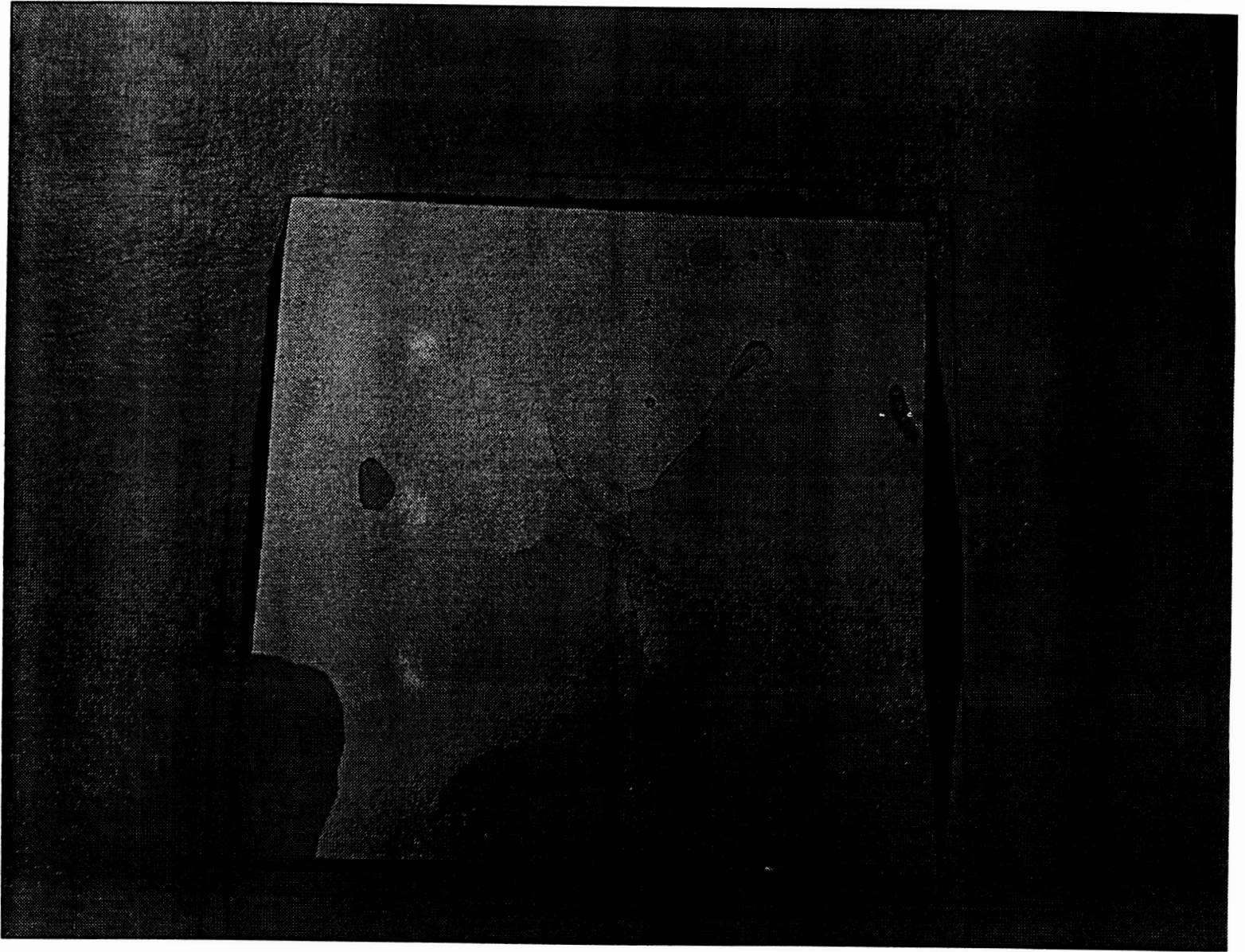


Figure 13: Crack pattern in the adhesive at a relatively lower load

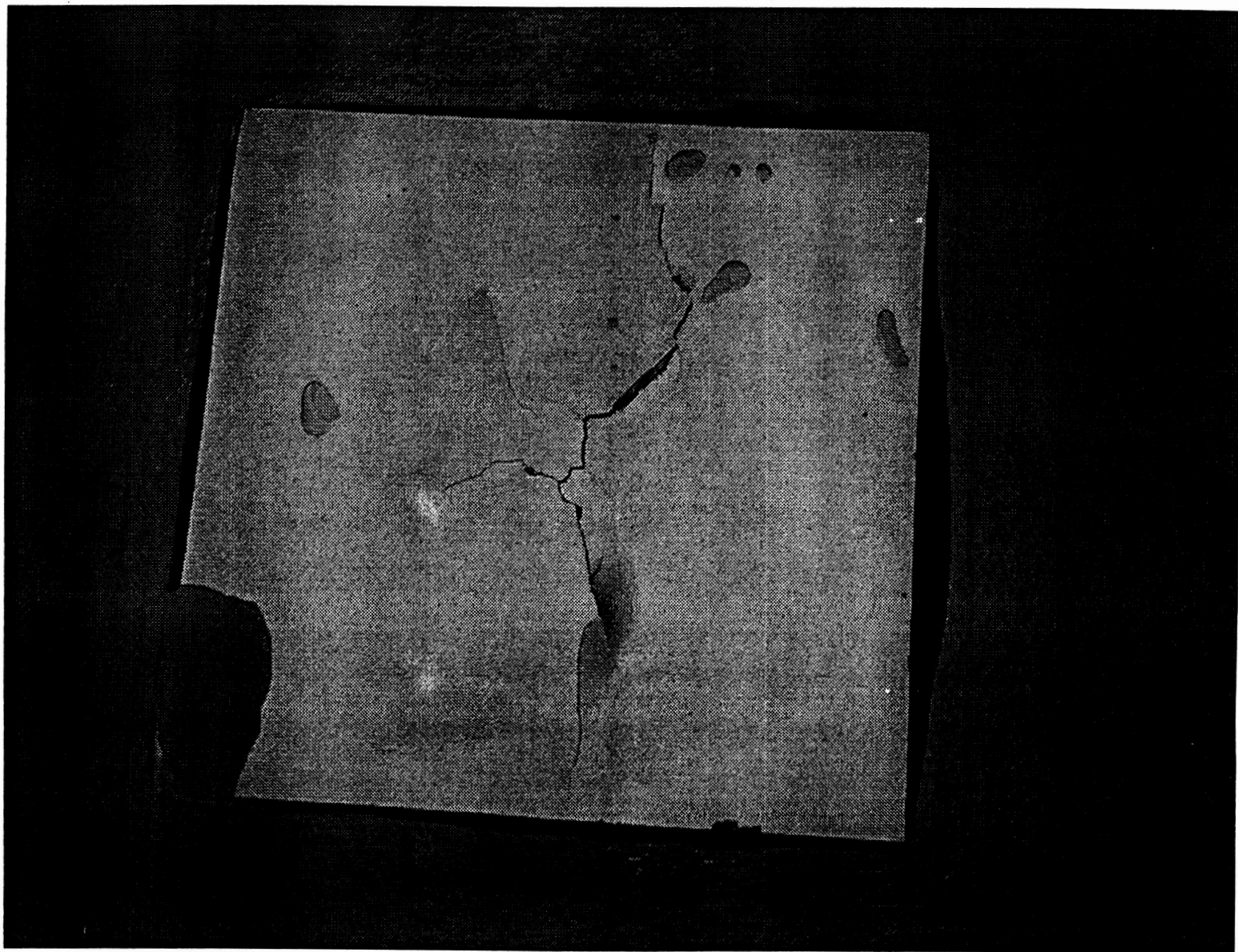


Figure 14: Crack pattern in the adhesive at a relatively higher load